Organic Electronics 13 (2012) 1086–1091

Contents lists available at SciVerse ScienceDirect

Organic Electronics

journal homepage: www.elsevier.com/locate/orgel

Efficient planar organic solar cells with the high near-infrared response

Weichao Chen [a,b], Lizhen Huang [a,b], Xiaolan Qiao [a,b], Jianbing Yang [a,b], Bo Yu [a], Donghang Yan [a,*]

[a] State Key Laboratory of Polymer Physics and Chemistry, Changchun Institute of Applied Chemistry, Chinese Academy of Sciences, Changchun 130022, PR China
[b] Graduate School of Chinese Academy of Sciences, Beijing 100039, PR China

ARTICLE INFO

Article history:
Received 29 November 2011
Received in revised form 13 February 2012
Accepted 3 March 2012
Available online 22 March 2012

Keywords:
Organic solar cells
Near-infrared
Titanyl phthalocyanines
EQE

ABSTRACT

Efficient planar organic solar cells extending the response into the near-infrared (NIR) were fabricated using the highly ordered Titanyl phthalocyanines (TiOPc) films as the donor layer. This type of films obtained through the weak epitaxy growth (WEG) method presents good continuity and integrity with the low density of grain boundaries. More importantly the films own a strong absorption in the NIR (750–950 nm) and a broad absorption spectrum from 550 to 950 nm. Meanwhile the high external quantum efficiency (EQE) is obtained in the NIR with the peak value over 38% and the EQE is over 18% in the entire response range, which could benefit from the long exciton diffusion length and the high carrier mobility of the highly ordered films. Thereby the fabricated planar solar cells achieve a high short-circuit current density (J_{sc}) of 9.26 mA cm^{-2} and a power conversion efficiency (PCE) of 2.67%.

1. Introduction

Organic solar cells have attracted extensive attention due to the low cost, light weight and flexibility. Their power conversion efficiency advances considerably since the Tang reported the donor–acceptor planar solar cell [1], but the efficiency is still not enough for industrialization compared with the solar cells based on the silicon. One limiting factor is the inadequate utilization of the solar spectrum. Typically the absorption range of the current materials used for organic solar cells is located in the visible region [2–6], but over 40% solar energy falls into the NIR. Thereby two-cell integration by series or parallel (One main response lies in visible region and the other in NIR) could be an optimal option to solve the limitation [7,8]. The devices with the main response in the visible region have been done well [9,5,6], and much attention recently is paid to the devices extending the response into the NIR [10–18]. Based on these current research outcomes, it is crucial to design the films showing the strong absorption in the NIR and enabling the improvement of the cells performance.

TiOPc is a typical non-planar phthalocyanine, one of the most sensitive organic photoconductors in the NIR. Its absorption spectrum, photoconductivity and charge-transport properties all depend on a variety of the phases. Specifically the phase II has a shorter separated distance between adjacent molecules than the phase I [19,20,13] and it enhances the intermolecular π–π interaction. The phase II TiOPc has been proven to be an excellent *p*-type semiconductor with high photoconductivity, and correspondingly the film possesses a broad absorption spectrum and the strong absorption in the NIR. Thus the film is more appropriate one as the donor layer in the cell. Much work has been done to fabricate directly the phase II films on the different substrates (KBr, indium tin oxide (ITO) glass, and sapphire, and oriented poly(tetrafluoroethylene)) [21,22] or to adopt diverse approaches (supersonic molecular bean epitaxy and organic molecular beam deposition) [21-24]. These films, composed of separated crystallites, are inappropriately applicable to the solar cells, and the phase II films which can be used in the solar cells are often obtained by the indirect method [13]. The method includes two steps: the amorphous films are obtained firstly

* Corresponding author.
E-mail address: yandh@ciac.jl.cn (D. Yan).

1566-1199/$ - see front matter © 2012 Elsevier B.V. All rights reserved.
http://dx.doi.org/10.1016/j.orgel.2012.03.002

by vacuum deposition on the ITO substrate at room temperature, and then treated by solvent annealing for several hours. This process, however, is supposed to be complex for fabricating the solar cells. The small grains and many grain boundaries in the films would cause the low carrier mobility and high density of traps which restrict the cell performance. As is reported, the exciton diffusion length (L_D) can be improved by enhancing the order of the films [25]. Therefore it is necessary to prepare directly the highly ordered TiOPc films which can be used as the donor layer in the cells.

In this paper, we report a type of planar solar cells extending the response into the NIR by using the highly ordered phase II TiOPc films as the donor layer. Through the WEG technique [26], the films are prepared with the 2,5-bis(4-biphenylyl)-bithiophene (BP2T) as the inducing layer. The epitaxial relationship formed between phase II TiOPc and BP2T generates highly ordered and continuous TiOPc films. They present a broad response range from 550 to 950 nm and a strong absorption in the NIR (750–950 nm). Meanwhile the high carrier mobility in the films could favor the exciton separation and the carrier transport [27]. Thereby the fabricated planar solar cells (BP2T/TiOPc/C_{60}) achieve a high J_{sc} of 9.26 mA cm^{-2} and a PCE of 2.67%.

2. Experiment

2.1. Materials and device fabrication

The TiOPc, C_{60} and 8-hydroxyquinoline aluminum (Alq3) were purchased from Aldrich Corp, and BP2T was synthesized according to the reference [28]. The chemical structures of TiOPc and BP2T are shown in Fig. 1(a). Prior to deposition, all the organic compounds were purified twice via thermal-gradient sublimation.

The ITO-coated glasses with a sheet resistance of 10 Ω sq^{-1} were wiped with detergent, ultrasonic treatment in acetone, alcohol and deionized water in sequence and subsequently dried in pure N_2. Then they were coated with a 40 nm thick poly(3,4-ethylenedioxythiophene):poly(styrene sulfonic acid) (PEDOT:PSS) by spin coating. Afterwards the substrates were dried at 160 °C for 15 min in air. BP2T and TiOPc were deposited sequentially on the substrate which was kept at 160 °C (T_{sub} = 160 °C), then C_{60}, Alq3 and Al on it at room temperature. The area of the cathode is defined by a shadow mask with an active area of 3.14 mm^2. In the process of deposition, the pressure remains below 10^{-4} Pa, the rate below 0.1 nm s^{-1} for organic materials and 1 nm s^{-1} for Al. For comparison, we also prepared the cells with TiOPc films obtained under different conditions. The vertical diodes were fabricated to estimate the carrier mobility.

2.2. Characterization of films and device measurements

The film morphologies were imaged by a SPI 3800/SPA 300HV (Seiko Instruments Inc., Japan) with tapping mode. The selected area electron diffraction was taken by JEOL JEM-1011 transmission electron microscope operated at 100 kV. The wide angel X-ray diffraction (XRD) patterns were performed in a D8 discovery thin-film diffractometer with Cu $K\alpha$ radiation (=1.54056). The selected voltage and current were 40 kV and 40 mA respectively.

The current–voltage curves of the solar cells were measured by a Keithley 2400 source-measurement under 100 mW cm^{-2} illuminations (SS150W solar simulator, Sciencetech Inc.) calibrated with a standard silicon cell traced to the National Renewable Energy Laboratory (NREL). The EQE was measured with Q Test Station 2000 (Crowntech Inc. USA). The current–voltage tests of diodes were also taken with a Keithley 2400 source-measurement at room temperature in air.

3. Results and discussion

3.1. Film morphologies, structural properties and absorption spectra

Fig. 1(b) shows the atomic force microscope (AFM) topography image of the 20 nm TiOPc films on the 8 nm BP2T (TiOPc/BP2T). The TiOPc/BP2T films composed of lamellar crystals demonstrate a layer-by-layer growth behavior, and the lamellar crystals are intimately coalesced with each other. Consequently the films present good continuity and integrity with the low density of grain boundaries. It differs greatly from the morphology of TiOPc grown directly on the ITO substrate (TiOPc/ITO). The TiOPc/ITO films are composed of small-sized and randomly-oriented spherical grains with denser grain boundaries as seen in Fig. 1(c). The induction of the BP2T enhances the continuity and integrity of the TiOPc films and subtracts the grain boundaries.

The out-of-plane X-ray diffraction patterns of the TiOPc films are shown in Fig. 1(d). The strong intensity diffraction peak is found in the TiOPc/BP2T films which is located at 7.5° corresponding to the (010) lattice plane of the phase II TiOPc films. It indicates these films are highly ordered. However, the TiOPc films deposited onto the ITO substrate are amorphous or poor crystalline, because there is no visible diffraction peak.

Selected area electron diffraction was performed to investigate the in-plane relationships between TiOPc and BP2T. The epitaxial relationship is found between TiOPc and BP2T. In Fig. 1(f), the diffraction spots of TiOPc are indexed into (001) and (−2 −12) of the phase II. There are three in-plane orientations of TiOPc in each domain of BP2T corresponding to incommensurate epitaxy and commensurate epitaxy respectively. For incommensurate epitaxy, the angle of $(-2\,-12)_{TiOPc\text{-}2}$ and $(-2\,-12)_{TiOPc\text{-}3}$ with respect to b^*_{BP2T} is ±55° respectively. For commensurate epitaxy, evidenced by the coincidence of $(-2\,-12)_{TiOPc\text{-}1}$ and $(020)_{BP2T}$, the relationship is as follows: $(010)_{TiOPc}$//$(001)_{BP2T}$, $[101]_{TiOPc}$//$[010]_{BP2T}$. The WEG mechanism leads to the highly in-plane orientation and the compact stack of TiOPc molecules on the BP2T layer, which can explain the layer-by-layer growth behavior. The WEG relationship also improves the order of the films.

Fig. 2 illustrates the normalized absorption spectra. Specifically the TiOPc/ITO films manifest a peak at 720 nm with a shoulder centered at 650 nm, which is consistent with the amorphous TiOPc films [21]. However, the TiOPc/BP2T

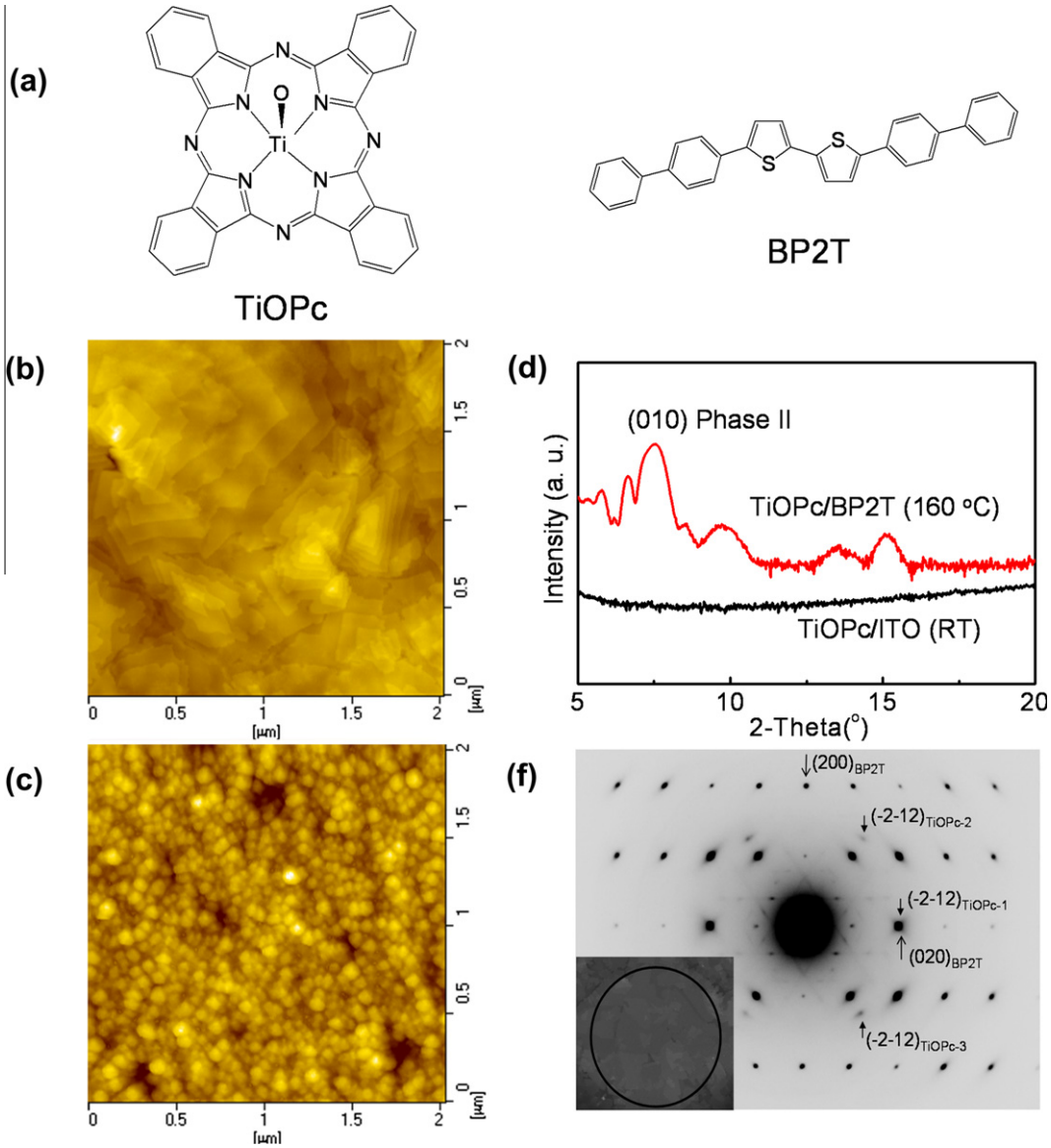

Fig. 1. (a) Molecular structures of TiOPc and BP2T. (b) and (c) AFM topography images of the TiOPc (20 nm)/BP2T (8 nm) films (2 × 2 μm) and TiOPc (15 nm)/ITO films (2 × 2 μm) respectively. (d) X-ray diffraction spectra of the TiOPc/BP2T films and TiOPc/ITO films. (f) Selected area electron diffraction (SAED) pattern of the TiOPc/BP2T films.

films demonstrate an extremely different absorption spectrum compared with the TiOPc/ITO films and show a typical absorption spectrum of the phase II TiOPc films obtained at the high temperature [23,22]: the broad absorption range, the strong absorption in the NIR and the relatively weak absorption in the visible region. The differences of the absorption spectrum could be made by a variety of molecular packing in the two types of the films. The phase II TiOPc has the strong intermolecular π–π interaction [20], which can result in the red shift of the absorption spectrum. Additionally the TiOPc/BP2T films exhibit a more red-shift intense peak at 870 nm and correspondingly a broader absorption range from 550 to 950 nm, compared with the TiOPc films in phase II obtained by solvent annealing treatment [13]. It may be due to the improvement of the TiOPc's order in the TiOPc/BP2T films which has been confirmed by the XRD as seen in the Fig. 1(d). This type of large-area, highly ordered and continuous films which present the broad response and the strong absorption in the NIR is an alternative for fabricating the tandem solar cells.

3.2. Device performance

Owing to the inducement of BP2T, the large-area and highly ordered TiOPc films have been fabricated, and subsequently the planar solar cells based on the films were constructed. For comparison, the cells with the TiOPc/ITO films were also prepared. The current density–voltage

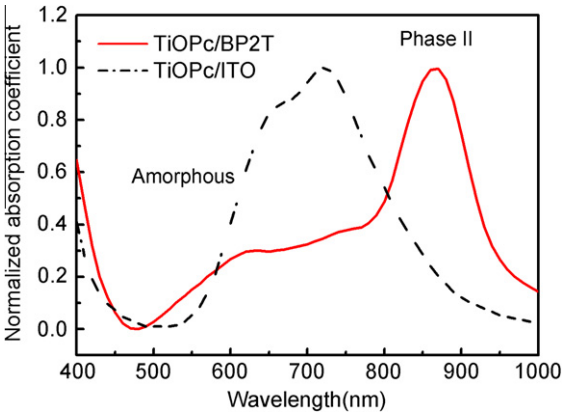

Fig. 2. The absorption spectra of TiOPc (20 nm)/BP2T (8 nm) films and TiOPc (15 nm)/ITO films.

(*J*–*V*) curves of the ITO/PEDOT:PSS (40 nm)/BP2T (8 nm)/TiOPc (20 nm)/C_{60} (40 nm)/Alq3 (5 nm)/Al (T_{sub} = 160 °C) (BP2T/TiOPc/C_{60}) and ITO/TiOPc (15 nm)/C_{60} (40 nm)/Alq3 (5 nm)/Al (T_{sub} = room temperature (RT)) (TiOPc/C_{60}) cells under the light illumination are imaged in Fig. 3(a) with the device configurations inset. The device performance parameters were summarized in Table 1. Obviously, the BP2T/TiOPc/C_{60} cells exhibit much better performance than the TiOPc/C_{60} cells: the higher J_{sc} (9.26 mA cm^{-2}) and fill factor (*FF*) (0.6). In order to define what affects the performance of the devices, the devices with different structures are also fabricated as follows:

Cell A: ITO/PEDOT:PSS (40 nm)/TiOPc (15 nm)/C_{60} (40 nm)/Alq3 (5 nm)/Al (T_{sub} = RT)
Cell B: ITO/PEDOT:PSS (40 nm)/BP2T (8 nm)/TiOPc (15 nm)/C_{60} (40 nm)/Alq3 (5 nm)/Al (T_{sub} = RT)
Cell C: ITO/PEDOT:PSS (40 nm)/TiOPc (15 nm)/Alq3 (5 nm)/Al (T_{sub} = 160 °C).

By comparing the performance of the three devices (TiOPc/C_{60}, Cell A and Cell B) in the Table 1, it indicates that the introduction of PEDOT:PSS and BP2T cannot improve the performance of the devices at room temperature. And the Cell C without BP2T also does not perform well at 160 °C, although the J_{sc} is improved slightly. Inferably the introduction of BP2T at 160 °C could effectively improve the performance of the cells. This may be that the BP2T improves the order of the crystalline TiOPc films, which can affect the L_D and the carrier mobility. As shown in Fig. 3(b), the improvement of the J_{sc} in the BP2T/TiOPc/C_{60} cells is owing to the high EQE of over 18% in the entire response range, especially in the NIR with the peak value of 38%. The high EQE value from 780 to 910 nm is realized due to the strong absorption of the TiOPc/BP2T films in the NIR where the TiOPc/ITO films hardly have absorption. Integrating the EQE curve of the BP2T/TiOPc/C_{60} cells from 400 to 950 nm with the standard AM 1.5G solar spectrum, a current density about 8.76 mA cm^{-2} is obtained, which is slightly lower than the measured value (9.26 mA cm^{-2}) with the error <5%. The photocurrent from the contribution of TiOPc is about 5.95 mA cm^{-2} by integrating the response

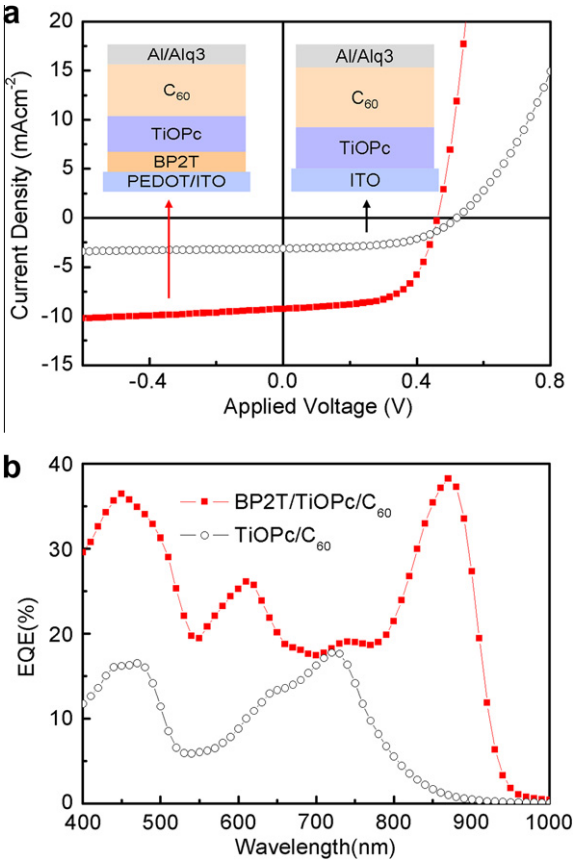

Fig. 3. (a) The typical current density (*J*)–voltage (*V*) curves of the ITO/PEDOT:PSS (40 nm)/BP2T (8 nm)/TiOPc (20 nm)/C_{60} (40 nm)/Alq3 (5 nm)/Al and ITO/TiOPc (15 nm)/C_{60} (40 nm)/Alq3 (5 nm)/Al cells under the light illumination with the device configurations inset. (b) The corresponding EQE curves of the devices respectively.

from 550 to 950 nm. The integration of the response in the NIR from 750 to 950 nm yields the current density of 3 mA cm^{-2} which offers 50% of the current density from TiOPc. The high response in the NIR is a crucial factor for the improvement of the J_{sc}. On the other hand, the BP2T/TiOPc/C_{60} cells manifest higher EQE values than the TiOPc/C_{60} cells in the entire response range. It could be attributed to the long L_D and the high carrier mobility of the ordered TiOPc/BP2T films. The L_D is estimated using the transfer matrix method with the optical interference effect according to the references [29,30]. By fitting the EQE curves of the BP2T/TiOPc/C_{60} cells and the TiOPc/C_{60} cells, the L_D of the TiOPc/BP2T is approximately 19 nm which is higher than that of the TiOPc/ITO films (9 nm). The increase of L_D could benefit from the enhanced order of the TiOPc/BP2T films. Details of the effects have been discussed in another place [31]. The carrier mobility of the vertical direction in the TiOPc films was measured with the device structures of ITO/PEDOT/BP2T/TiOPc (100 nm)/Au (T_{sub} = 160 °C) and ITO/TiOPc (100 nm)/Au (T_{sub} = RT) using a space-charge-limited-current model. The typical *J*–*V* curves are presented in Fig. 4 with the device configures inset. The ordered TiOPc/BP2T films have the high vertical mobility (2.2×10^{-4} cm^2 V^{-1}s^{-1}), which is one order

Table 1
Device parameters for organic solar cells based on TiOPc/C_{60} heterojunctions.

Device structures	V_{oc}[a] (V)	J_{sc} (mA cm^{-2})	*FF*	PCE (%)
ITO/PEDOT:PSS/BP2T/TiOPc/C_{60}/Alq3/Al (160 °C)	0.48	9.26	0.60	2.67
ITO/TiOPc/C_{60}/Alq3/Al (RT)	0.52	3.12	0.54	0.88
ITO/PEDOT:PSS/TiOPc/C_{60}/Alq3/Al (RT)	0.52	2.54	0.31	0.41
ITO/PEDOT:PSS/BP2T/TiOPc/C_{60}/Alq3/Al (RT)	0.52	2.98	0.41	0.64
ITO/PEDOT/TiOPc/C_{60}/Alq3/Al (160 °C)	0.26	4.18	0.35	0.38

[a] The open-voltage.

of magnitude higher than the amorphous TiOPc/ITO films (1.3×10^{-5} cm^2 V^{-1}s^{-1}). The TiOPc/BP2T films with high order and good continuity supply the high carrier mobility [26], which can improve the transport efficiency and consequently boost the EQE [30].

It is acknowledged that the response from 400 to 550 nm is the contribution of C_{60}. In the BP2T/TiOPc/C_{60} cells, the response of C_{60} is larger than that of TiOPc/C_{60} cells. It indicates that the ordered TiOPc films can improve the separation efficiency of excitons generated in the C_{60} layer, given the same condition of C_{60} deposition. The high carrier mobility is proven to raise the exciton separation efficiency [27]. Thus the high EQE from 400 to 550 nm might be due to the high carrier mobility in the films. Meanwhile the high carrier mobility possibly decreases the series resistance (R_s) of the devices. The BP2T/TiOPc/C_{60} cell has a lower R_s (1.44 Ω cm^2) than TiOPc/C_{60} cell (4.82 Ω cm^2). Also the low density of the traps in the TiOPc/BP2T films could decrease the carrier recombination. Thereby the BP2T/TiOPc/C_{60} cell has the higher *FF* (0.6).

In conclusion, we have fabricated efficient planar organic solar cells based on the highly ordered TiOPc films obtained through the WEG technique. The films are prepared by the inducing of BP2T directly. Composed of lamellar crystals connecting with each other, the films show good continuity and integrity which decrease the density of grain boundaries. On the other hand, the films manifest the strong absorption in the NIR (750–950 nm) with the broad response from 550 to 950 nm. Thus the cells using these films as the donor layer and C_{60} as the acceptor achieve a broad response from 400 to 950 nm with the EQE over 18%. Moreover, the higher EQE in the NIR is obtained with the peak value of over 38% at 870 nm, and correspondingly the cells yield a PCE of 2.67% with a high J_{sc} of 9.26 mA cm^{-2} and *FF* (0.6). This work also provides an optimal option for fabricating multi-component solar cells to realize the broad spectral coverage into the NIR.

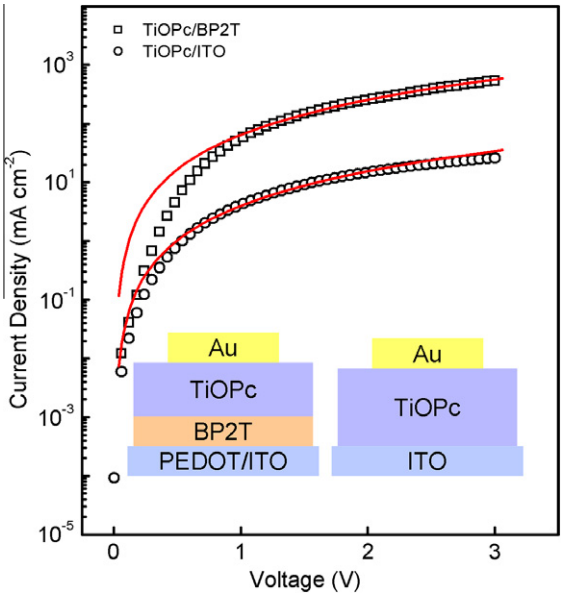

Fig. 4. The typical current density (*J*)–voltage (*V*) curves of the ITO/PEDOT/BP2T/TiOPc (100 nm)/Au (T_{sub} = 160 °C) and ITO/TiOPc (100 nm)/Au (T_{sub} = RT) diodes with the device configurations inset. The symbols are experimental data for transport of holes, and the solid lines are fitted according to the space-charge-limited-current model.

Acknowledgements

This work was financially supported by the National Natural Science Foundation of China (51133007) and The National Basic Research Program (2009CB939702).

References

[1] C.W. Tang, 2-Layer organic photovoltaic cell, Appl. Phys. Lett. 48 (1986) 183–185.
[2] P. Peumans, S.R. Forrest, Very-high-efficiency double-heterostructure copper phthalocyanine/C-60 photovoltaic cells, Appl. Phys. Lett. 79 (2001) 126–128.
[3] S. Yoo, B. Domercq, B. Kippelen, Efficient thin-film organic solar cells based on pentacene/C-60 heterojunctions, Appl. Phys. Lett. 85 (2004) 5427–5429.
[4] B. Yu, L.Z. Huang, H.B. Wang, D.H. Yan, Efficient organic solar cells using a high-quality crystalline thin film as a donor layer, Adv. Mater. 22 (2010) 1017–1020.
[5] Z. He, C. Zhong, X. Huang, W.-Y. Wong, H. Wu, L. Chen, S. Su, Y. Cao, Simultaneous enhancement of open-circuit voltage, short-circuit current density, and fill factor in polymer solar cells, Adv. Mater. 23 (2011) 4636–4643.
[6] D.H. Wang, K.H. Park, J.H. Seo, J. Seifter, J.H. Jeon, J.K. Kim, J.H. Park, O.O. Park, A.J. Heeger, Enhanced power conversion efficiency in PCDTBT/PC(70)BM bulk heterojunction photovoltaic devices with embedded silver nanoparticle clusters, Adv. Energy Mater. 1 (2011) 766–770.
[7] J.Y. Kim, K. Lee, N.E. Coates, D. Moses, T.Q. Nguyen, M. Dante, A.J. Heeger, Efficient tandem polymer solar cells fabricated by all-solution processing, Science 317 (2007) 222–225.
[8] A.P. Yuen, A.M. Hor, J.S. Preston, R. Klenkler, N.M. Bamsey, R.O. Loutfy, A simple parallel tandem organic solar cell based on metallophthalocyanines, Appl. Phys. Lett. 98 (2011) 173301.
[9] Y. Matsuo, Y. Sato, T. Niinomi, I. Soga, H. Tanaka, E. Nakamura, Columnar structure in bulk heterojunction in solution-processable three-layered p-i-n organic photovoltaic devices using tetrabenzoporphyrin precursor and silylmethyl[60]fullerene, J. Am. Chem. Soc. 131 (2009) 16048–16050.

[10] B.P. Rand, J.G. Xue, F. Yang, S.R. Forrest, Organic solar cells with sensitivity extending into the near infrared, Appl. Phys. Lett. 87 (2005) 233508.
[11] R.F. Bailey-Salzman, B.P. Rand, S.R. Forrest, Near-infrared sensitive small molecule organic photovoltaic cells based on chloroaluminum phthalocyanine, Appl. Phys. Lett. 91 (2007) 013508.
[12] J.G. Dai, X.X. Jiang, H.B. Wang, D.H. Yan, Organic photovoltaic cells with near infrared absorption spectrum, Appl. Phys. Lett. 91 (2007) 253503.
[13] D. Placencia, W.N. Wang, R.C. Shallcross, K.W. Nebesny, M. Brumbach, N.R. Armstrong, Organic photovoltaic cells based on solvent-annealed, textured titanyl phthalocyanine/C(60) heterojunctions, Adv. Funct. Mater. 19 (2009) 1913–1921.
[14] K.V. Chauhan, P. Sullivan, J.L. Yang, T.S. Jones, Efficient organic photovoltaic cells through structural modification of chloroaluminum phthalocyanine/fullerene heterojunctions, J. Phys. Chem. C 114 (2010) 3304–3308.
[15] T. Sakurai, T. Ohashi, H. Kitazume, M. Kubota, T. Suemasu, K. Akimoto, Structural control of organic solar cells based on nonplanar metallophthalocyanine/C(60) heterojunctions using organic buffer layers, Org. Electron. 12 (2011) 966–973.
[16] K. Vasseur, B.P. Rand, D. Cheyns, L. Froyen, P. Heremans, Structural evolution of evaporated lead phthalocyanine thin films for near-infrared sensitive solar cells, Chem. Mater. 23 (2011) 886–895.
[17] B. Verreet, R. Müller, B.P. Rand, K. Vasseur, P. Heremans, Structural templating of chloro-aluminum phthalocyanine layers for planar and bulk heterojunction organic solar cells, Org. Electron. 12 (2011) 2131–2139.
[18] W. Wang, D. Placencia, N.R. Armstrong, Planar and textured heterojunction organic photovoltaics based on chloroindium phthalocyanine (ClInPc) versus titanyl phthalocyanine (TiOPc) donor layers, Org. Electron. 12 (2011) 383–393.
[19] L.Q. Li, Q.X. Tang, H.X. Li, X.D. Yang, W.P. Hu, Y.B. Song, Z.G. Shuai, W. Xu, Y.Q. Liu, D.B. Zhu, An ultra closely pi-stacked organic semiconductor for high performance field-effect transistors, Adv. Mater. 19 (2007) 2613–2616.
[20] J.E. Norton, J.L. Bredas, Theoretical characterization of titanyl phthalocyanine as a p-type organic semiconductor: Short intermolecular pi–pi interactions yield large electronic couplings and hole transport bandwidths, J. Chem. Phys. 128 (2008) 034701.
[21] H. Yonehara, H. Etori, M.K. Engel, M. Tsushima, N. Ikeda, T. Ohno, C. Pac, Fabrication of various ordered films of oxotitanium(IV) phthalocyanine by vacuum deposition and their spectroscopic behavior, Chem. Mater. 13 (2001) 1015–1022.
[22] M. Brinkmann, J.C. Wittmann, M. Barthel, M. Hanack, C. Chaumont, Highly ordered titanyl phthalocyanine films grown by directional crystallization on oriented poly(tetrafluoroethylene) substrate, Chem. Mater. 14 (2002) 904–914.
[23] A. Yamashita, T. Maruno, T. Hayashi, Phase-selective formation of titanylphthalocyanine thin-films by organic molecular-beam deposition, J. Phys. Chem. 98 (1994) 12695–12701.
[24] K. Walzer, T. Toccoli, A. Pallaoro, R. Verucchi, T. Fritz, K. Leo, A. Boschetti, S. Iannotta, Morphological and optical properties of titanyl phthalocyanine films deposited by supersonic molecular beam epitaxy (SuMBE), Surf. Sci. 573 (2004) 346–358.
[25] R.R. Lunt, J.B. Benziger, S.R. Forrest, Relationship between crystalline order and exciton diffusion length in molecular organic semiconductors, Adv. Mater. 22 (2010) 1233–1236.
[26] H.B. Wang, F. Zhu, J.L. Yang, Y.H. Geng, D.H. Yan, Weak epitaxy growth affording high-mobility thin films of disk-like organic semiconductors, Adv. Mater. 19 (2007) 2168–2171.
[27] L.M. Andersson, C. Muller, B.H. Badada, F.L. Zhang, U. Wurful, O. Inganas, Mobility and fill factor correlation in geminate recombination limited solar cells, J. Appl. Phys. 110 (2011) 024509.
[28] S. Hotta, H. Kimura, S.A. Lee, T. Tamaki, Synthesis of thiophene/phenylene co-oligomers. II. Block and alternating co-oligomers, J. Heterocycl. Chem. 37 (2000) 281–286.
[29] L.A.A. Pettersson, L.S. Roman, O. Inganas, Modeling photocurrent action spectra of photovoltaic devices based on organic thin films, J. Appl. Phys. 86 (1999) 487–496.
[30] P. Peumans, A. Yakimov, S.R. Forrest, Small molecular weight organic thin-film photodetectors and solar cells, J. Appl. Phys. 93 (2003) 3693–3723.
[31] J.B. Yang, F. Zhu, B. Yu, H.B. Wang, D.H. Yan, Simultaneous enhancement of charge transport and exciton diffusion in single-crystal-like organic semiconductors, Appl. Phys. Lett. 100 (2012) 103305.